

# Ultrasonic Treatment of Soybean Protein Isolate: Unveiling the Mechanisms for Gel Functional Improvement and Application in Chiba Tofu

Xiao Wu,<sup>†</sup> Na Li,<sup>†</sup> Zeng Dong, Qin Yin, Marwan M. A. Rashed, Lixiang Zhu, Chuanlong Dan, Xinyue Li, Ziping Chen,<sup>\*</sup> and Kefeng Zhai<sup>\*</sup>



Cite This: *ACS Omega* 2024, 9, 44588–44600



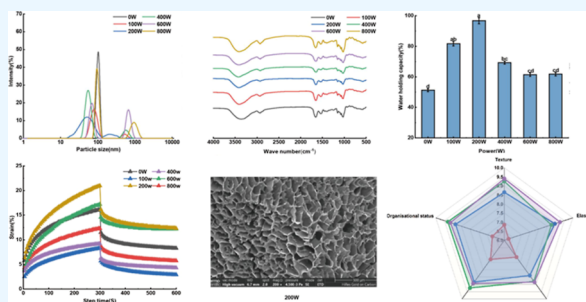
Read Online

ACCESS |

Metrics & More

Article Recommendations

**ABSTRACT:** Soybean protein isolate (SPI) cannot meet the needs of modern food production due to various shortcomings. By change of its structural characteristics, its application in the food field may be increased. This study explored the impact of ultrasonic treatment on the structural and gelation properties of the SPI dispersions. By subjecting SPI to ultrasonic treatment at 0–800 W for 10 min, it was found that this treatment significantly reduced the particle size of SPI to 196 nm and caused an increase in its solubility, surface hydrophobicity, and sulfhydryl content as well as significant changes in the protein structure. At an optimal ultrasonic power of 200 W, SPI gels demonstrated an enhanced gelling ability, strength, and water-holding capacity, forming a more uniform and compact structure. Application in Chiba tofu showed that water retention, elasticity, and sensory quality were optimized at 200 W. The findings highlight that a sonication power of 200 W significantly improves the physicochemical and structural properties of SPI, resulting in a denser and more functional gel suitable for Chiba tofu production.



## 1. INTRODUCTION

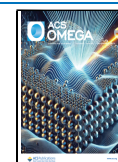
Soybean, a globally cultivated oilseed, is a crucial source of vegetable protein for human consumption.<sup>1</sup> Soy isolate protein (SPI) is a full-value protein product derived from low-temperature defatted soybean meal.<sup>2</sup> SPI is a product known for its affordability and high protein content and extensively used in food processing. However, it is often challenging for natural SPI to meet the specific needs of modern food production, such as low solubility,<sup>3</sup> deterioration of gelatinization,<sup>4</sup> low digestibility,<sup>5,6</sup> and poor foam stability.<sup>7</sup> These limitations hinder the further development and applications of SPI in the food industry and significantly restrict its application in the field of foodstuffs.<sup>8</sup> Therefore, exploring efficient and safe modification methods of SPI, improving the functional properties of soybean protein, and increasing the added value of soybean protein have become a hotspot of concern for many experts and scholars in the food field.<sup>9,10</sup>

The methods to improve the functional properties of SPI mainly include physical, chemical, and enzymatic modifications.<sup>11</sup> Among these techniques, ultrasonic technology is a common physical modification technique widely used in the field of auxiliary ingredient extraction.<sup>8,12</sup> It is characterized by simplicity, energy-saving, time-saving, and environmental protection<sup>13</sup> and is based on cavitation and mechanical and thermal effects generated by low-frequency oscillation.<sup>14</sup> In recent years, ultrasound research has focused on the use of

ultrasound for the modification and degradation of various biomolecules. Ultrasound induces structural changes by disrupting noncovalent interactions and can even break peptide bonds, as well as cause changes in their functional properties.<sup>15</sup> Wang et al. induced SPI gel by ultrasonic-assisted calcium salts.<sup>16</sup> Liu et al. carried out ultrasonic modification of peanut isolate proteins. They found that ultrasonic waves can reduce the particle size of peanut isolate proteins, change the structure of proteins, and improve the solubility and emulsification of peanut proteins.<sup>17</sup> Ultrasonic technology has excellent potential in protein modification and new product development due to its advantages of being fast and efficient, safe, and reliable.<sup>18,19</sup> However, not much research has been done on the application of modified SPI in traditional food processing.

Therefore, SPI was modified by ultrasonic treatment in this study. The changes in the structure and gel properties of SPI were analyzed by particle size, free sulfhydryl content, and

**Received:** July 31, 2024  
**Revised:** October 9, 2024  
**Accepted:** October 17, 2024  
**Published:** October 23, 2024



surface hydrophobicity analysis; endogenous fluorescence spectroscopy and Fourier transform infrared (FT-IR) spectroscopy; textural structure; and scanning electron microscopy (SEM) testing. Then, the modified SPI was applied to Chiba tofu in the hope that the effect of ultrasonic treatment on the SPI and its enhanced gel is more clearly elaborated, providing certain theoretical support for the application of SPI in food, which is of great significance for its development process and wide application in the industrialization of food processing.

## 2. MATERIALS AND METHODS

**2.1. Materials.** Soybean protein isolate (SPI, SD201, protein content  $\geq 90\%$ ) was purchased from Shanghai Xintai Food Ingredients Mall (Shanghai, China), and glutamine aminotransferase (enzyme activity 100 U/g) was purchased from Beijing Solebao Biotechnology Co., Ltd. (Beijing, China). Jinluo Chiba tofu was purchased from Linyi Xincheng Jinluo Meat Products Group (Linyi, China). All chemical reagents used were of analytical grade.

**2.2. Preparation of Ultrasonically Treated SPI Dispersion Samples.** Six sets of SPI solutions with a mass concentration of 3 g/100 mL were prepared in a 50 mL beaker, and the mixture was stirred for 3 h until fully dissolved. The ultrasonic treatment of SPI dispersion was done using an ultrasonic input power of (0, 100, 200, 400, 600, and 800 W) for 10 min (with a pulse mode of 9 s on and 9 s off) with an ultrasonicator (Scientz-IIID, Ningbo Scientz Biotechnology Co. Ltd., Ningbo, China). An ice bath was used to cool the temperature during the ultrasonication process, and the probe was maintained at 1–2 cm below the surface of the SPI solution during sonication. Then, the dispersed solution was placed in a refrigerator at 4 °C for 12 h, 15 mL was taken and poured into a Petri dish, and placed at –80 °C for prefreezing and freeze-drying, and the samples used for the determination of all the indicators were kept for 5 days.<sup>20</sup>

**2.3. Physicochemical Properties of SPI Dispersion after Ultrasonic Treatment.** **2.3.1. Particle Size Measurements.** The concentration of the prepared dispersion was diluted to about 1 mg/mL with deionized water for measurement. 1.2 mL of the desired sample was weighed for each measurement, and the particle size of the dispersion was determined using an LD-DLS90 laser particle size analyzer.<sup>21,22</sup>

**2.3.2. Solubility.** The samples were diluted to approximately 5 mg/mL using deionized water and adjusted to pH 7, and then the protein content was determined by the Bis-urea method. 1 mL of the dispersion sample was mixed well with 4 mL of Bis-urea reagent, and then the measurement wavelength was set to 540 nm on a UV spectrophotometer to determine its absorbance.<sup>23,24</sup> The samples were then centrifuged for 15 min at 25 °C and 8000 rpm, the supernatant was subjected to the same treatment, and the absorbance value was measured again at 540 nm. The protein concentration was calculated by substituting the measured absorbance value into the bovine serum albumin (BSA) standard curve. Protein solubility was the ratio of the protein content in the supernatant to the total protein content.

**2.3.3. Surface Hydrophobicity.** The surface hydrophobicity of proteins was determined with reference to the ANS (8-aniline-1-naphthalenesulfonic acid) method.<sup>25</sup> The ANS solution was prepared to 8 mM by adding 10 mM, pH 7.0, phosphate buffer. The sonicated SPI dispersion was diluted to about 5 mg/mL with deionized water, followed by centrifugation of the diluted samples for 15 min at a parameter

setting of 4 °C and 10,000g. The supernatant was extracted, and the protein content was determined by the bis(2-hydroxyurea) method.<sup>23</sup> The SPI solution was diluted with deionized water at 0.005, 0.01, 0.05, 0.1, 0.3, and 0.5 mg/mL. Then, 2 mL of the diluted solution was mixed well with 10  $\mu$ L of ANS solution. The fluorescence intensity was measured using a multifunctional enzyme marker, the excitation wavelength was set at 365 nm, and the emission wavelength was set at 484 nm. The resulting fluorescence intensity value was fitted to the protein content measured by the bisulfite reagent method, and the value of the initial slope in the resulting linear fit was the magnitude of the surface hydrophobicity of the corresponding SPI dispersion samples.<sup>15,26</sup>

**2.3.4. Sulfhydryl Content.** The total sulfhydryl content was measured as described by Li et al. (2023) with some modification.<sup>27</sup> The samples were prepared to a concentration of 2% (w/v), and 1 mL of the solution was removed and treated with 8 mL of Tris-glycine solution (pH 8.0, Tris-HCl 10.4 g, EDTA 1.2 g, glycine 6.9 g, and urea 480 g), followed by homogenization and centrifugation at 10,000 rpm for 15 min, to remove the insoluble proteins. 4.5 mL of the supernatant and 0.5 mL of 10 mmol/L Ellman reagent were reacted (this reagent consisted of 4 mg of DTNB/mL in pH 8.0 Tris-glycine buffer), and 4.5 mL of Tris-glycine and 0.5 mL of 10 mmol/L Ellman reagent were used as a blank sample with a reaction time of 30 min. Afterward, the absorbance values were measured spectrophotometrically at 412 nm.<sup>28</sup> The protein content of the dissolved samples was determined using the bisulfite method, the blank control was used without protein solution, the absorbance value at 540 nm was determined, and the protein solution was obtained according to the standard curve equation. The formula is calculated as follows

$$\begin{aligned} \text{Total sulfhydryl content } (\mu\text{mol/L/mg}) \\ = [(A_1 - A_2 - A_3) \times V_1] / [(\varepsilon \times C \times L) \times V_2] \times 100\% \end{aligned} \quad (1)$$

where  $A_1$  is the absorbance of the measuring tube,  $A_2$  is the absorbance of the blank tube,  $A_3$  is the absorbance of the control tube,  $V_1$  is the total volume of the reactants, mL,  $\varepsilon$  is the molar extinction coefficient of 13,600  $\text{M}^{-1}\cdot\text{cm}^{-1}$ ,  $C$  is the protein content,  $L$  is the optical diameter (0.5 cm), and  $V_2$  is the sample volume, mL.

**2.4. Structural Properties of SPI Dispersion after Ultrasonic Treatment.** **2.4.1. FT-IR Spectroscopy Analysis.** 1–2 mg of lyophilized sample and 200 mg of KBr were fully ground and mixed. After pressurizing at 150 MPa for 5 min, the infrared spectra of the samples were collected by using a Fourier infrared spectrometer.<sup>29</sup> The parameters were set as follows: wavelength range: 4000–400  $\text{cm}^{-1}$  and scanning times: 32. Data analysis was processed using PeakFit software, and the percentage of protein secondary structure was calculated.

**2.4.2. Analysis of Endogenous Fluorescence Spectra.** The fluorescence spectra in the SPI samples were determined using an SH-6600 fluorescence spectrophotometer, and the samples were dispersed in phosphate buffer with a concentration of 0.01 mol/L and pH 7.0. The protein solution was prepared to a suitable concentration with an excitation wavelength of 290 nm and the scanned emission spectral range of 300–400 nm for fluorescence spectral analysis.<sup>30,31</sup>

**2.4.3. SDS-PAGE Gel Electrophoresis.** SPI and conjugate samples were analyzed by SDS-PAGE using a 12% separator gel and 5% concentrate gel. Samples with a protein content of 5 mg/mL were mixed 1:1 with Laemmli sample buffer containing 5% (v/v) mercaptoethanol. Subsequently, the samples were heated in a water bath at 95 °C for 5 min and then centrifuged at 10,000g for 15 min, and the supernatant was collected for electrophoresis. The electrophoresis sample was 15 L, and a constant voltage of 125 V was loaded onto the gel. The gel was eluted in a dish, fixed with fixative for 30 min, stained with staining solution for 30 min, and then decolorized.<sup>32,33</sup>

**2.5. Preparation of SPI-Enhanced Gel by Ultrasonic Treatment.** SPI solution with a mass concentration of 18 g/100 mL was prepared in a 50 mL beaker and stirred for 3 h until fully dissolved, and the soy protein solution was ultrasonicated by using a probe. An ice bath was used to cool the temperature during the sonication process, and the ultrasonic frequency was 0, 100, 200, 400, 600, and 800 W, and the ultrasonic time was 10 min. Every 9 s of ultrasonication, the ultrasonication was stopped for 9 s; the pH value of ultrasonicated samples was adjusted to 6.9, and then, the samples were left to stand in refrigeration for 2 h. After heating in a water bath at 95 °C for 10 min, the TG enzyme was added at 0.90 U/g, and the samples were incubated in a water bath at 50 °C. The enzyme was held at 50 °C water bath conditions for 1 h, 75 °C inactivation of the enzyme 15 min immediately after the cooling of the ice bath, refrigerated overnight, and then demolded, standby.<sup>34–36</sup>

**2.6. Physicochemical Properties of Gels.** **2.6.1. Determination of Gel Water-Holding Capacity.** About 2 g of the gel was weighed as  $W_1$ , then wrapped in filter paper, placed in a centrifuge tube, and centrifuged at 8000 rpm for 10 min. After centrifugation, the filter paper was removed, and the gel on the filter paper was carefully scraped off and weighed as  $W_2$ . The following formula calculated the water-holding capacity of the gel<sup>37,38</sup>

$$\text{WHC (\%)} = W_2/W_1 \times 100\% \quad (2)$$

**2.6.2. Gel Textural Properties.** The TMS-PRO mass spectrometer and P/0.5 probe were used for the determination of TPA on the SPI gels. The tested gels were 30 mm high and 25 mm in diameter.<sup>39</sup> The test conditions are set as follows: force sensing element range 40 N, probe height above the sample back up 60 mm, deformation amount 50%, detection speed 30 mm/min, and starting force 0.075 N. Finally, the samples were placed on the stage to be tested and measured after the end of the measurement to save the experimental data in the gel adhesion data and analyze the processing.<sup>40</sup>

**2.6.3. Gel Strength.** The gel strength was measured with a TMS-PRO mass spectrometer using a P/0.5 probe. To avoid damage, the gel was not removed from the beaker during measurement. The probe was punctured at 1 mm/s with a detection rate of 30 mm/min and a trigger force of 0.075 N.<sup>41,42</sup>

**2.6.4. Gel Solubility.** The gel samples were dissolved in four different buffer solutions: (A) deionized water, adjusted to pH 8.0; (B) Tris-gly buffer (0.086 M Tris, 0.09 M glycine, and 4 mM Na<sub>2</sub>EDTA, pH 8.0); (C) buffer B dissolved in 8 M urea and 0.5% sodium dodecyl sulfate (SDS), pH 8.0; and (D) buffer C dissolved in 10 mM dithiothreitol (DTT), pH 8.0. The mixtures were shaken at room temperature and then shaken to 8000 mM. pH 8.0; (D) buffer C was dissolved in 10

mM dithiothreitol (DTT), pH 8.0. The mixture was shaken at room temperature and centrifuged at 8000 rpm for 2 min. The supernatant was taken, the absorbance value was measured at 750 nm, and the protein content was obtained according to the BSA standard curve.<sup>43,44</sup>

$$\text{Protein solubility (\%)} = M_1/M_2 \times 100\% \quad (3)$$

where  $M_1$  is the protein in the supernatant, mg, and  $M_2$  is the total protein content, mg.

Note: Solution Tris-gly buffer disrupts electrostatic interactions; urea is capable of disrupting noncovalent bonding interactions such as hydrophobic and hydrogen bonds; SDS is closely associated with hydrophobic amino acids; and DTT acts as a strong reducing agent and is capable of breaking disulfide bonds (S–S).

**2.7. Gel Rheology.** The prepared gels were placed on an MCR102 rheometer, a 40 mm diameter flat plate fixture was selected, the strain was set to 1%, the samples were subjected to frequency scanning in the frequency range of 0.1–100 rad/s, and the temperature was set to 25 °C. The changes of  $G'$ ,  $G''$ , and  $\tan \delta$  with frequency were measured.<sup>45</sup> Creep and recovery tests were performed at 25 °C under a shear stress of 5 Pa. Constant stress was applied for 300 s, and the recovery response was applied for 300 s.<sup>46</sup>

**2.8. DSC Measurements.** 2.0 mg portion of each freeze-dried gel powder was weighed accurately and pressed in an aluminum box and then measured by DSC using an empty aluminum box as a blank control. The temperature range was 20–150 °C, the heating rate was 10 °C/min, the flow rate of nitrogen was 20 mL/min, and the DSC scanning curve was obtained.<sup>47–49</sup>

**2.9. SEM Measurements.** The SEM measurements were performed by taking a certain mass of freeze-dried SPI gel samples and placing on the conductive gel on the slide, removing the scattered gel powder, transferring the samples into the ion sputtering apparatus and vacuum gold spraying for a while, then observing the samples under the electron microscope, selecting the magnification as 200 times, adjusting the appropriate area in order to observe the morphology of the gel, and taking photographs clearly.<sup>50,51</sup>

**2.10. Application to Chiba Tofu.** **2.10.1. Preparation of Chiba Tofu.** First, 15 g of SPI and 80 mL of water were taken in a clean beaker, stirred well, then sonicated at 200 W ultrasonic power for 10 min, and then poured into a blender at the end of the process. Then, 5 g of starch, 0.135 g of glutamine aminotransferase, 2 g of soybean oil, and 0.5 g of salt were added successively, and the slurry was mixed rapidly for 2 min until uniform and then mixed slowly for about 5 min to make the slurry uniform and fine, without bubbles. Finally, the batter was poured into the tray, about 4 cm thick, and the surface was covered with plastic wrap and refrigerated at 4 °C for 10 h to set. At the end of refrigeration, the tofu was steamed at 80–85 °C for 40 min, so that the center temperature was higher than 75 °C, and then cooled and cut into cubes to obtain the desired sample of Chiba tofu.

As described above, unmodified SPI was used to produce unmodified Chiba tofu, which was cut and set aside. In addition, two other brands of tofu (Shengfa and Jinluo) purchased from the market were used as control samples.

**2.10.2. Water-Holding Capacity of Chiba Tofu.** Chiba tofu was cut into cubic pieces with a knife, and the mass  $W_1$  (about 2 g) of Chiba tofu was accurately weighed into a 50 mL centrifuge tube, wrapped in filter paper, and then centrifuged

in the centrifuge tube (8000 rpm, 10 min). After centrifugation, we removed the filter paper from the centrifuge tube, carefully scraped the tofu off the paper, and weighed the mass of centrifuged tofu,  $W_2$ . The water-holding capacity of the tofu was calculated according to the following formula<sup>38</sup>

$$\text{WHC (\%)} = W_2/W_1 \times 100\% \quad (4)$$

**2.10.3. Elasticity of Chiba Tofu.** The TPA of Chiba tofu was determined using an FTC mass tester and a P/50 probe. The height of Chiba tofu was 30 mm, the length and width were 25 mm, and the test conditions were set as follows: the force sensing element range was 40 N, the height of the probe above the sample was 60 mm, the amount of deformation was 50%, the speed of detection was 30 mm/min, and the starting force was 0.075 N. Finally, the samples were placed on the table to be tested, the measurement was started, and the data were saved in the experimental data and analyzed. At the end of the measurement, the data on the elasticity of Chiba tofu were saved and analyzed.<sup>52,53</sup>

**2.10.4. Sensory Evaluation of Chiba Tofu.** Twenty people (10 male and 10 female) trained in specialized courses in food science were chosen to assess the sensory evaluation of each type of Chiba tofu according to the criteria in Table 1.<sup>54–56</sup>

**2.11. Data Processing.** All of the experiments were replicated 3 times, and the data were analyzed using Microsoft Excel 2023, PeakFit v4.12, and SPSS 20 statistical software. The significance of the difference was established at  $p < 0.05$ , and the results were expressed as calculated mean and standard deviation ( $M \pm SD$ ). Origin 2022 software was used for graphing.

### 3. RESULTS AND DISCUSSION

**3.1. Effect of Ultrasonic Treatment on the Physicochemical Properties of SPI Dispersions.** As shown in Figure 1A,B, the ultrasonic power of 100, 200, 400, and 600 W made the particle size of SPI decrease significantly ( $p < 0.05$ ). At the same time, there was no significant difference between 800 W and the control, but the value decreased. As shown in Figure 1A, the control sample was a single peak state, and 100 W was a bimodal distribution. The small particle size peaks accounted for the main part; 200 W ultrasound, the particle size was further reduced, and the small particle size peak area increased; 400 W ultrasound, the particle size increases, and the double peaks shifted to the significant direction of the particle size; 600 W ultrasound, the distribution of the two peaks tended to be close to the area of the two peaks; 800 W ultrasound was still a bimodal distribution, and the distribution of small particles was close to the control. As shown in Figure 1B, the average particle size of SPI after ultrasonic treatment was reduced compared to that of SPI without ultrasonic treatment. The average particle size decreased and then increased with the increase of ultrasonic power and reaches a minimum of 196 nm under ultrasonic treatment at 200 W. This is due to the fact that the dispersion of SPI is affected by the cavity effect generated by ultrasonic waves, resulting in turbulence. The turbulence is able to generate mechanical shear and resulting in the protein particles being chopped up. When the ultrasonic power is too high, there is an increase in the average particle size. It may be due to the fact that the protein particles are subjected to noncovalent bonding and form fine aggregates.<sup>57–59</sup>

As shown in Figure 1C, the surface hydrophobicity of SPI showed a tendency to increase and then decreased with the

Table 1. Sensory Evaluation Criteria for Chiba Tofu

items	texture	elasticity	taste	color	organizational status
good	smooth, delicate, and crisp (7–10 points)	very elastic, tough, and unbreakable by finger pressure (7–10 points)	fresh and tasty, with the inherent flavor of Chiba tofu (7–10 points)	have the normal color of Chiba tofu, uniform color (7–10 points)	smooth and even cut surface, no large air holes (7–10 points)
general	smoother and more delicate (4–6 points)	more elastic, not broken by finger pressure (4–6 points)	the inherent aroma of Chiba tofu, no off-flavor (4–6 points)	with the normal color of Chiba tofu, uneven color (4–6 points)	the cut surface is more even, with a few air holes (4–6 points)
wrong	not crisp, rough, and delicate (1–3 points)	poor elasticity, rupture by finger pressure (1–3 points)	no aroma of Chiba tofu, bad odor (1–3 points)	no Chiba tofu normal color (1–3 points)	cutting surface rough and uneven, loose (1–3 points)

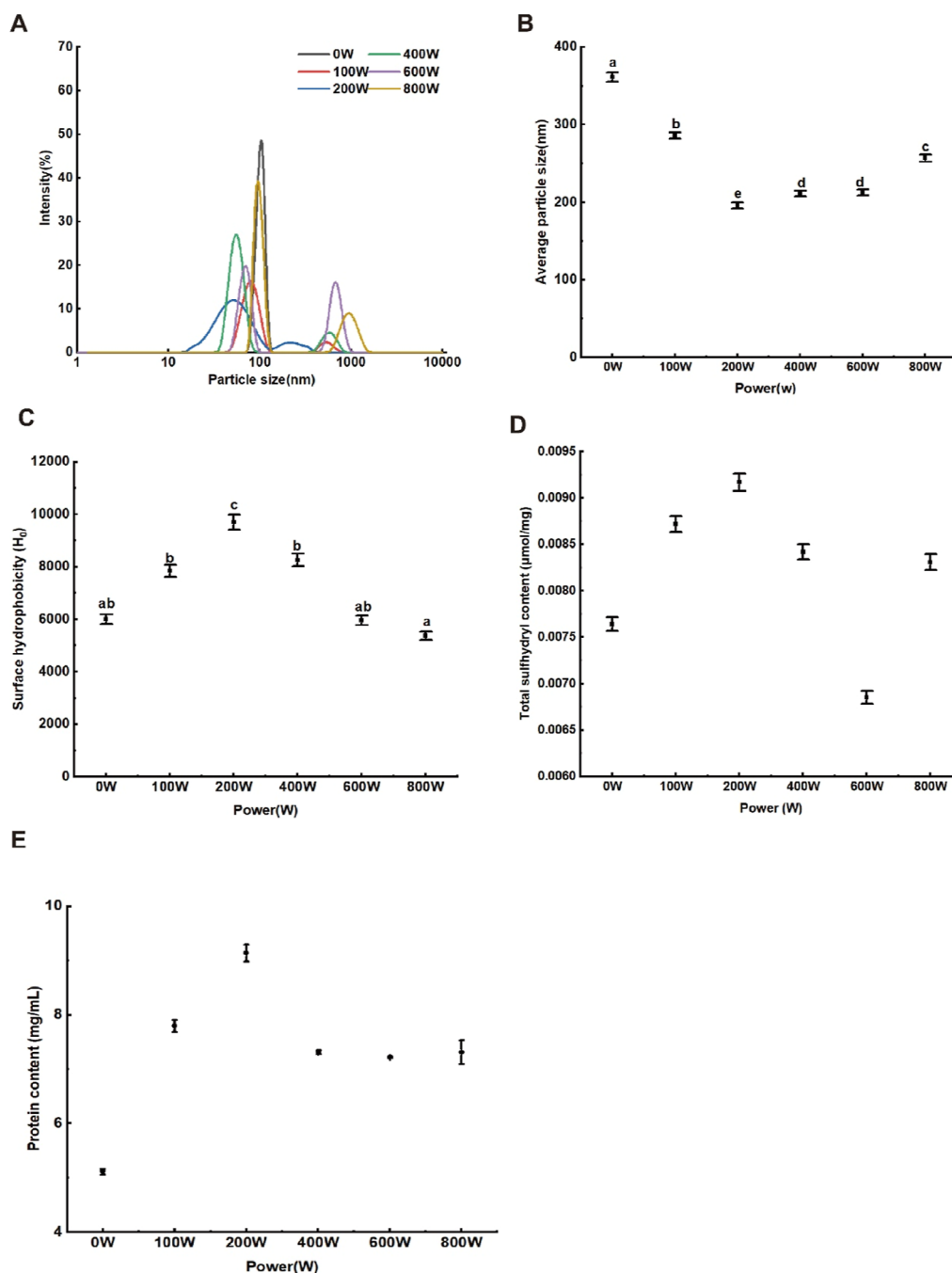


**Figure 1.** Graphs of results of physicochemical properties of SPI dispersions under different ultrasonic powers. (A) Average particle size distribution; (B) average particle size results; (C) surface hydrophobicity results; (D) total sulfhydryl content results; and (E) solubility between different solvents.

increase of ultrasonic power. It reached a maximum value of 9697.40 when the ultrasonic power was 200 W. This is due to the fact that ultrasonic treatment may expose the hydrophobic groups of the proteins, which may increase their surface hydrophobicity.<sup>60</sup> However, suppose that the power of the treatment is too high. In that case, the protein particles may be reaggregated due to noncovalent forces, which may cause the hydrophobic groups to be encapsulated again, leading to a decrease in the surface hydrophobicity.<sup>61,62</sup>

As shown in Figure 1D, the total sulfhydryl content of SPI dispersions showed a trend of increasing and then decreasing with the gradual increase in ultrasonication power. The total

sulfhydryl content reached the maximum value of 0.008781 mol/mg when the ultrasonication power was 200 W. This is because the internal structure of the protein was unfolded so that the sulfhydryl group increased; with the further increase of ultrasonic power, the sulfhydryl group content would decrease, probably because the disulfide bond appeared between peptide and peptide or molecule and molecule, or oxidation reaction occurred.<sup>63</sup>

As shown in Figure 1E, the protein content of SPI without ultrasonic treatment was 5.10 mg/mL. The solubility of SPI after ultrasonic treatment was significantly improved, and the protein content of SPI after ultrasonic treatment (100, 200,

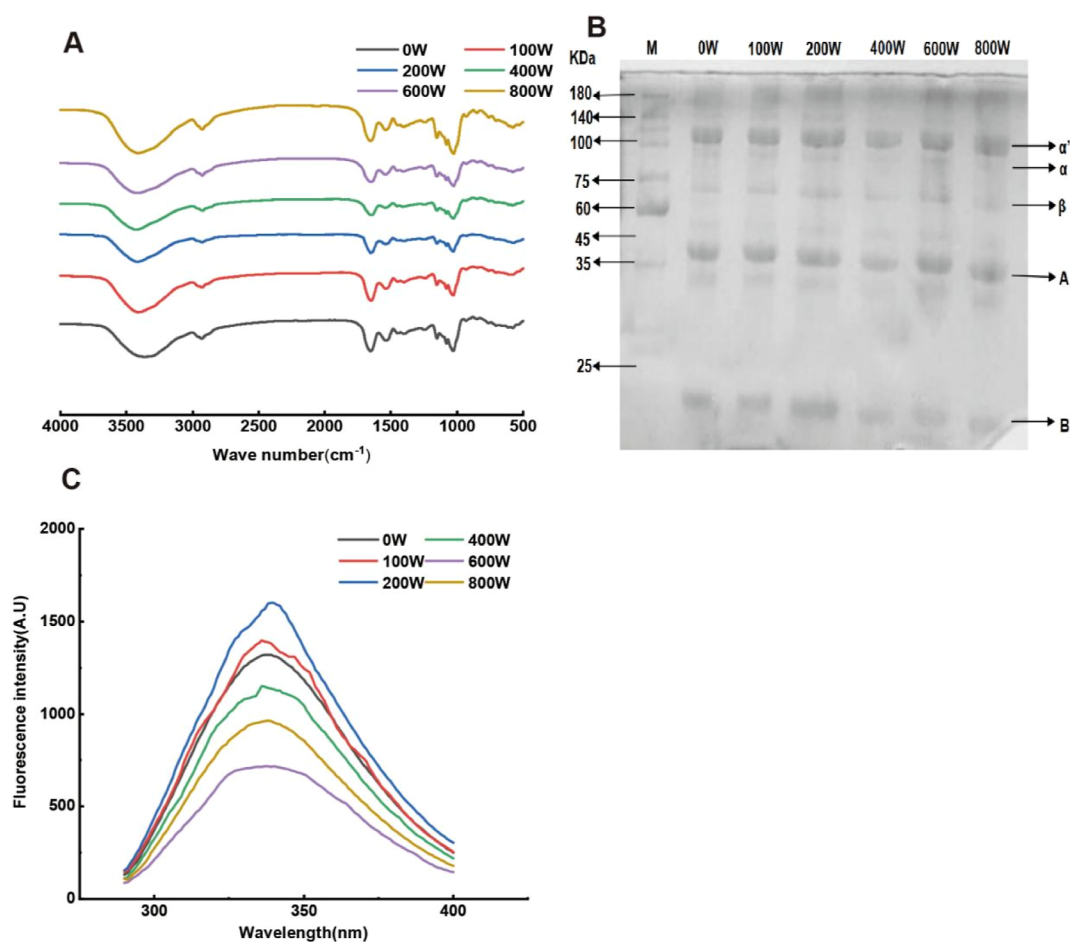


**Figure 2.** Plot of the results of SPI dispersion properties under different ultrasonic powers. (A) Endogenous fluorescence spectra; (B) electropherogram; and (C) FT-IR spectra.

**Table 2. Effect on SPI Secondary Structure after Ultrasonic Treatment<sup>a</sup>**

protein samples	components of the secondary structure (%)			
	$\alpha$ -helix	$\beta$ -folding	$\beta$ -corner	irregularly curled
0 W	0.46 $\pm$ 0.04 <sup>a</sup>	54.54 $\pm$ 0.75 <sup>a</sup>	44.73 $\pm$ 0.70 <sup>a</sup>	0.27 $\pm$ 0.03 <sup>a</sup>
100 W	0.40 $\pm$ 0.02 <sup>ab</sup>	54.85 $\pm$ 1.78 <sup>a</sup>	44.26 $\pm$ 0.62 <sup>a</sup>	0.50 $\pm$ 0.02 <sup>b</sup>
200 W	0.37 $\pm$ 0.04 <sup>b</sup>	54.76 $\pm$ 0.75 <sup>a</sup>	44.57 $\pm$ 0.71 <sup>a</sup>	0.30 $\pm$ 0.01 <sup>a</sup>
400 W	0.42 $\pm$ 0.01 <sup>ab</sup>	54.74 $\pm$ 0.31 <sup>a</sup>	44.57 $\pm$ 0.81 <sup>a</sup>	0.27 $\pm$ 0.03 <sup>a</sup>
600 W	0.44 $\pm$ 0.56 <sup>ab</sup>	54.35 $\pm$ 0.23 <sup>a</sup>	44.94 $\pm$ 0.45 <sup>a</sup>	0.27 $\pm$ 0.05 <sup>a</sup>
800 W	0.42 $\pm$ 0.02 <sup>ab</sup>	54.91 $\pm$ 0.38 <sup>a</sup>	44.15 $\pm$ 0.76 <sup>a</sup>	0.52 $\pm$ 0.04 <sup>b</sup>

<sup>a</sup>All values shown are mean  $\pm$  standard deviation. Dates with different letters (a and b) within a column indicate significantly different ( $p < 0.05$ ).

400, 600, and 800 W) was increased by 52.84%, 87.45%, 43.14%, 41.57%, and 43.53%, respectively; it can also be seen that with the increase of ultrasonic power, the protein solubility first increased and then slightly decreased, and at 200 W, the solubility reached a maximum of 9.56 mg/mL. Under the SPI dispersion ultrasonic power at 100 and 200 W treatment, the solubility continues to increase. The main reason may be the ultrasonic cavity bubbles and turbulence, etc., to be able to break up the protein molecular polymers. However, as the ultrasonic power was further increased, some aggregates were formed, which led to a decrease in solubility. Thus, ultrasonic treatment can reduce the size of protein aggregates and make them more susceptible to changes in water. At the same time, it changed the spatial configuration of proteins and affected their solubility in water.<sup>64</sup>

**3.2. Effect of Ultrasonic Treatment on the Structural Properties of SPI Dispersions.** As shown in Figure 2A, the data in Table 2 were obtained by processing and analyzing with PeakFit software. As can be seen from Table 2, after ultrasonic treatment, the relative content of the  $\alpha$ -helical structure of SPI decreased, the content of  $\beta$ -folding and  $\beta$ -turning did not change significantly, and the content of irregular curls increased significantly. The possible reason for this situation is that the secondary structure of proteins is mainly maintained by the hydrogen bonds between carbonyl and amide groups on the amino acids of the peptide chain. Moreover, the cavitation effect of ultrasound can disrupt these hydrogen bonding interactions. Then, the secondary structure of the protein molecule is damaged.<sup>13,67</sup> Therefore, it can be learned that

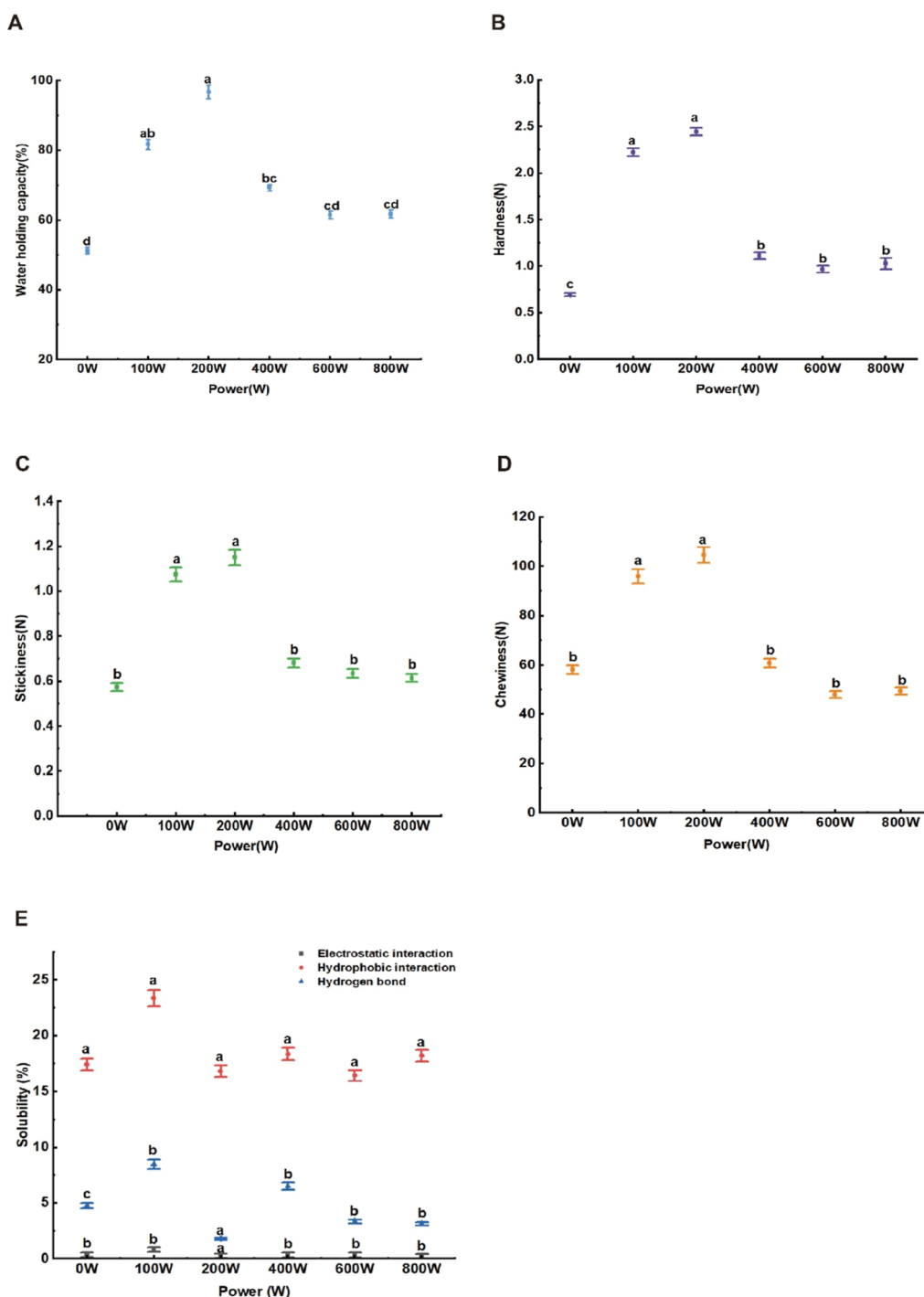


**Figure 3.** Resulting graphs of physicochemical properties of SPI gels under different ultrasonic powers. (A) Result graph of gel strength; (B) result graph of adhesion; (C) result graph of chewability; (D) result graph of water-holding property; and (E) solubility between different solvents.

ultrasonic treatment can destroy the secondary structure of SPI.

As shown in Figure 2B, after ultrasonic treatment, the electrophoretic bands of SPI all indicated that the A subunit and B subunit of soybean globulin and the  $\beta$ -subunit,  $\alpha'$ -subunit, and  $\alpha$ -subunit of companion soybean globulin were not damaged. This showed that the subunit structure of soybean isolates was not destroyed by a certain power of ultrasonication.<sup>66</sup>

As shown in Figure 2C, the unmodified SPI  $\lambda_{\max}$  is 337 nm, a very small degree of red shift occurs under the condition of

ultrasonic power 200 W, which indicates that under a certain ultrasonic power, the tryptophan chromophore group of the protein was exposed to the solvent, the protein molecules unfold, and its chromophore group was a hydrophobic group, which caused the hydrophobicity to increase. Under the condition of ultrasonic power 600 and 800 W. There was a very obvious decrease in the fluorescence intensity.<sup>30,31</sup> Under the conditions of 600 and 800 W ultrasonic power, the fluorescence intensity was obviously reduced, which indicated that the ultrasonic treatment could destroy the protein structure to a certain extent, causing the chromophore group

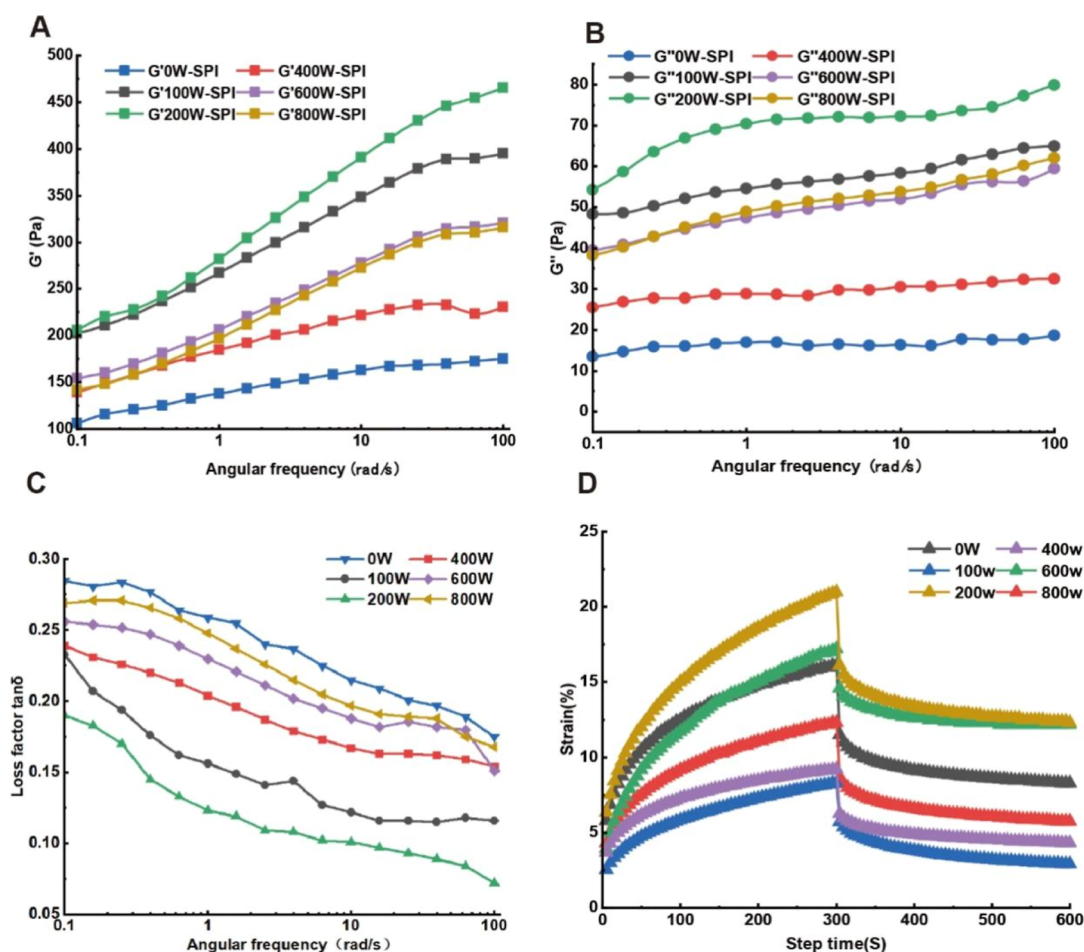


**Figure 4.** Effect of different ultrasonic power treatments on the rheological properties of SPI-formed gels. (A–C) Changes of energy storage modulus  $G'$ , loss modulus  $G''$ , and loss factor  $\tan \delta$  measured by frequency scanning, respectively; and (D) plot of creep and recovery results.

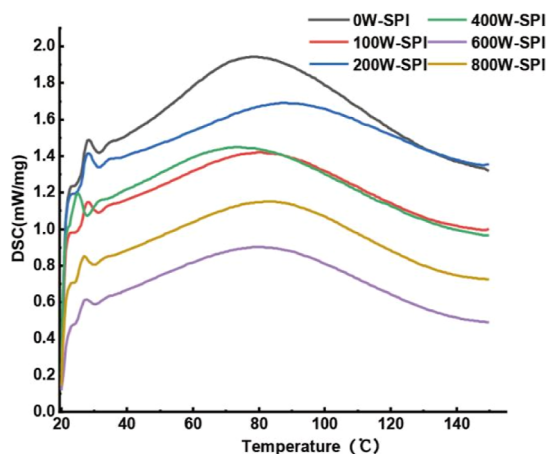


**Figure 5.** DSC scanning curves of SPI gels with different ultrasound powers.

to be exposed to the solvent, so the fluorescence intensity was reduced.<sup>65</sup>

**3.3. Effect of Ultrasonic Treatment on Physicochemical Properties of SPI-Forming Gels.** As shown in Figure 3A, the water-holding property of SPI gel showed a trend of increasing and then decreasing with the increase in ultrasonic power. The water-holding property of the gel formed by SPI was the highest at 96.68% at an ultrasonication power of 200

**Table 3. Thermal Stability of SPI Gels with Different Ultrasonic Powers<sup>a</sup>**

gel	peak temperature, $T_d/^\circ\text{C}$	heat content, $\Delta H/\text{J g}^{-1}$
0 W-SPI	$79.5 \pm 2.2^{\text{bc}}$	$184.4 \pm 2.46^{\text{a}}$
100 W-SPI	$80.6 \pm 2.1^{\text{bc}}$	$112.5 \pm 3.25^{\text{d}}$
200 W-SPI	$88.5 \pm 1.8^{\text{a}}$	$100.2 \pm 2.50^{\text{e}}$
400 W-SPI	$78.3 \pm 1.8^{\text{c}}$	$119.3 \pm 2.27^{\text{c}}$
600 W-SPI	$80.7 \pm 2.6^{\text{bc}}$	$125.0 \pm 2.66^{\text{b}}$
800 W-SPI	$82.9 \pm 2.0^{\text{b}}$	$123.6 \pm 2.44^{\text{bc}}$

<sup>a</sup>All values shown are mean  $\pm$  standard deviation. Dates with different letters (a–e) within a column indicate significantly different ( $p < 0.05$ ).

W. It indicated that ultrasonication can change the protein structure and promote the formation of network structure, which can effectively retain water and improve the water-holding property of the gel.<sup>68</sup>

As shown in Figure 3B, the strength of SPI gels reached the maximum at an ultrasonic treatment power of 200 W. This is because ultrasonic treatment destroyed part of the secondary structure of the protein, reduced the size of the protein particles, increased the surface area, and promoted the cross-linking modification of TG enzyme and SPI. When the ultrasonic power continued to increase, the protein molecular fragments were aggregated, their gel properties decreased, and the strength decreased.<sup>4,8</sup>



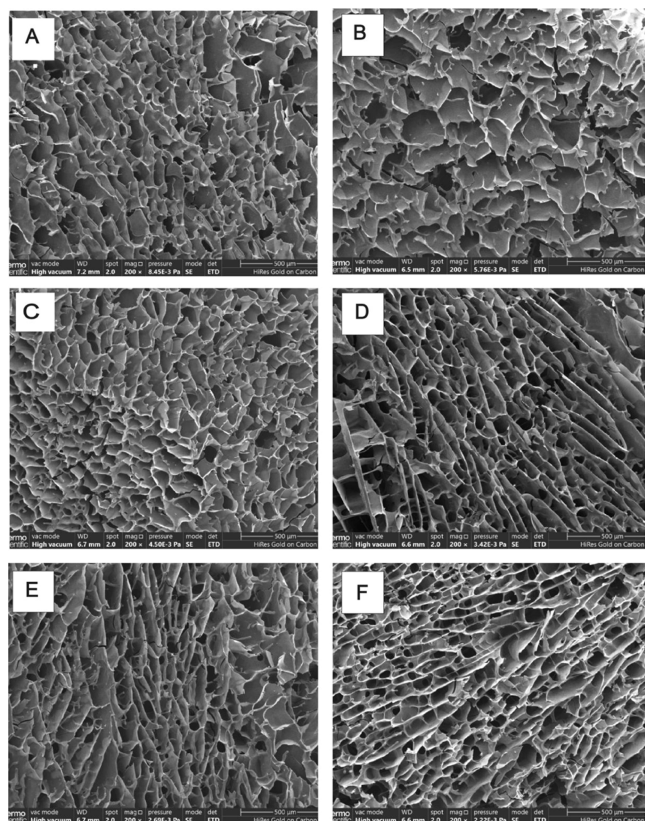


**Figure 6.** Scanning electron micrographs of SPI gels with different ultrasonic powers; (A) untreated gel; (B) 100 W treated gel; (C) 200 W treated gel; (D) 400 W treated gel; (E) 600 W treated gel; and (F) 800 W treated gel.

As shown in Figure 3C,D, the adhesive and masticatory properties of the SPI gels gradually increased and then leveled off with the increase of ultrasonic frequency. When the ultrasonic power was 200 W, the adhesive and masticatory properties of the gel reached a maximum of 1.15 and 104.63 N, respectively, which were 1.8 and 2 times higher than those of the SPI gel formed without ultrasonic treatment. It indicates that under 200 W ultrasonication, the hydrophobic groups of proteins were maximally exposed, the degree of cross-linking between protein molecules was the highest, and the gel network was finer, which contributed to the maximum adhesion and chewability of the gels.<sup>69,70</sup> As the ultrasonic power continued to increase, the gel structure of proteins would receive a certain degree of damage, making the gel adhesive and chewability decrease.

The difference in the gel solubility among the solvents indicated the magnitude of the intermolecular interaction forces, where solvents B and A represent electrostatic interactions, solvents C and B represent hydrophobic interactions, and solvents D and C represent hydrogen bonding interactions. Figure 3E shows the results of the intermolecular interaction forces of the gels produced under different ultrasonic power conditions. It can be seen that the structure of the gel network is mainly based on hydrophobic and hydrogen bonds, and the hydrophobic bonds play a non-negligible role in maintaining the gel structure. However, the solubility of the gel in the solvent was not very high and reached its lowest at 200 W of sonication. This phenomenon may be due to the formation of the  $\epsilon$ -( $\gamma$ -glutaminy)lysine

covalent bond between protein molecules catalyzed by the TG enzyme, which is 20 times stronger than that of hydrophobic and hydrogen bonds, and it can be assumed that this covalent bond is the main force of this gel network.<sup>2,34</sup> The lower solubility of the gel in the solvent indicated the higher contribution of this bond. The  $\epsilon$ -( $\gamma$ -glutaminy)lysine bond was the main force to maintain the ultrasound-modified gel network, followed by the hydrophobic bond and hydrogen bond.

#### 3.4. Effect of Ultrasonic Treatment on the Rheology of SPI-Forming Gels.

As shown in Figure 4A,B, the  $G'$  and  $G''$  of all gel samples showed an increasing trend with increasing time. Under partial ultrasonic power treatment, both  $G'$  and  $G''$  of the gel samples were higher than those of the untreated samples and were more obvious in the case of 200 W treatment, which indicates that ultrasonic treatment can increase the viscoelasticity of the gel and can lead to the formation of dense, homogeneous, and high-strength structure of the gel network formed by SPI.<sup>71</sup> Meanwhile, when the ultrasonic treatment power is 200 W, the  $\tan \delta$  value of the gel reached the lowest. It indicated that the network structure of the gel was less viscous, more elastic, and had a better three-dimensional mesh structure. Meanwhile, according to Figure 4D, the recovery rate of the gel formed by SPI under 200 W ultrasonic power treatment was the largest, 65.10%, which indicated that the mutual displacement between the gel chains under 200 W as ultrasonic treatment was serious. Due to the internal formation of huge friction, the structure was not easy to destroy and easier to recover. Therefore, in summary, the SPI gel treated with ultrasound has stronger elasticity and a more stable structure.

#### 3.5. Effect of Ultrasonic Treatment on the Thermal Stability of SPI-Forming Gels.

The DSC test curves of the freeze-dried samples of SPI gels and curve data are shown (Figure 5 and Table 3). The testing instrument we used was DSC214 (NETZSCH, Germany), and the DSC curve measured by this instrument indicated an endothermic process when the peak was upward. When the SPI sample was heated, the hydrogen bonds of SPI were broken, the energy was absorbed, and the protein molecules were changed from an ordered state to a disordered state, leading to the expansion of the protein molecules, which was the thermal denaturation process. We can also see that the  $T_d$  and  $\Delta H$  of the gel samples treated with different ultrasonic powers have obvious differences. The more significant peak temperature ( $T_d$ ) indicates the higher structural stability of the measured proteins, and the enthalpy ( $\Delta H$ ) is inversely proportional to the degree of protein denaturation, which can be used as a judgment indicator of the degree of denaturation of the proteins. 200 W ultrasonication, the gel reached the highest peak temperature of  $88.5 \pm 1.8$  °C, which was significantly higher than other ultrasonic power groups, which indicates that 200 W ultrasonication can enhance the thermal stability of the gel. However, the enthalpy ( $\Delta H$ ) had the opposite trend. The  $\Delta H$  of the nonultrasonicated SPI gel samples was  $184.4 \pm 2.46$  J  $g^{-1}$ . The  $\Delta H$  of the ultrasonicated gel samples was significantly reduced. The  $\Delta H$  of the 200 W ultrasonicated gel samples was the lowest among the samples, only  $100.2 \pm 2.50$  J  $g^{-1}$ , which showed that ultrasonication could lead to the denaturation of some of the soybean protein isolates. In contrast, the 200 W treatment could lead to the denaturation of some soybean protein isolates. This indicated that ultrasonic treatment can lead to the denaturation of some soybean protein isolates and

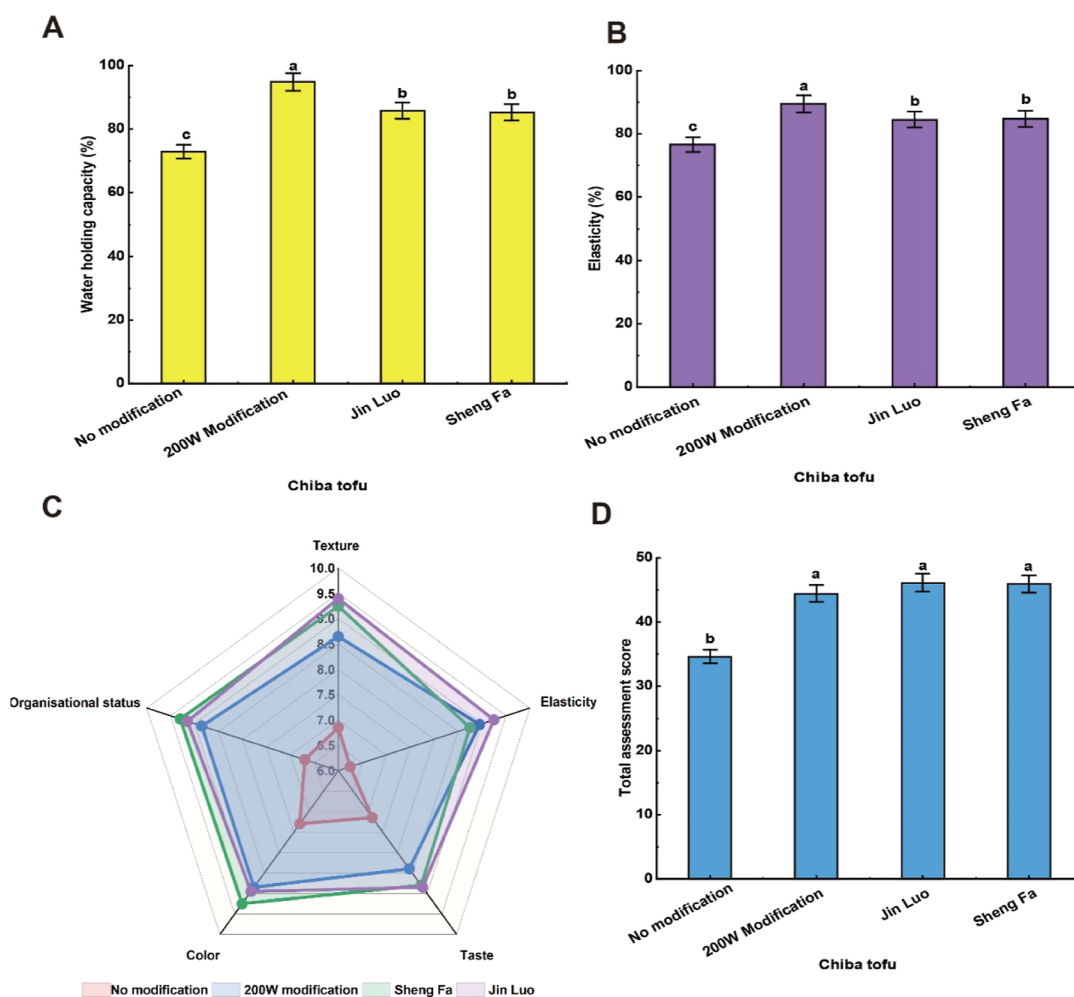


**Figure 7.** Measurement of physicochemical indexes of Chiba tofu and its sensory evaluation results. (A) Water-holding capacity, (B) elasticity, and (C,D) sensory evaluation results of Chiba tofu.

that the protein denaturation after the 200 W treatment was the deepest.

**3.6. Effect of Ultrasonic Treatment on the Structural Characterization of SPI Gel Formation.** The SEM results of the freeze-dried samples of SPI gels are shown in Figure 6, and a comparison shows that the 200 W ultrasound-treated gels formed a homogeneous, dense, smaller pore size, and neater reticulation structure. The improvement of gel strength and water retention is reflected macroscopically, which is consistent with the previous study. The reason may be that ultrasonication reduces the protein particle size and promotes TG cross-linking; ultrasonication unfolds the protein molecules and exposes more reactive groups, which promotes the formation of intermolecular disulfide bonds and hydrophobic interactions, and resulting in the formation of a homogeneous and dense gel structure. We have also conducted extensive experiments during the gel formation process of SPI. All the experiments proved that ultrasonic waves at 200 W for 10 min can improve the gelling ability, strength, and water retention capacity of SPI gels and form a more uniform and compact structure.

**3.7. Determination of Physicochemical Indexes of Chiba Tofu and Analysis of Its Sensory Evaluation Results.** As shown in Figure 7A, the water-holding property of Chiba tofu made from SPI after 200 W ultrasonic treatment was  $94.85 \pm 1.35\%$ , that of Chiba tofu made without treatment

was  $72.95 \pm 3.30\%$ , that of Chiba tofu made from two brands purchased from the market was around 85%, and that of Chiba tofu made from SPI after 200 W ultrasonic treatment significantly increased ( $p < 0.05$ ); thus, it can be seen that 200 W ultrasonic treatment of soybean protein isolates in the process of making Chiba tofu can significantly improve the water-holding property, which makes the quality of Chiba tofu better. The water-holding capacity of the 200 W ultrasonically treated SPI was significantly increased ( $p < 0.05$ ). These results indicated that the 200 W ultrasonication process of SPI can significantly improve the water-holding capacity of Chiba tofu and make the quality of Chiba tofu superior.

As shown in Figure 7B, the elasticity of Chiba tofu made from soybean protein isolates after 200 W ultrasonic treatment was  $89.47 \pm 1.18\%$ . The elasticity of unprocessed Chiba tofu was  $76.59 \pm 1.81\%$ . The elasticity of the two brands of Chiba tofu purchased on the market was about 84%. The elasticity of the SPI made from 200 W ultrasonication was significantly increased ( $p < 0.05$ ). These results showed that 200 W ultrasonication of soybean protein isolates in the process of making Chiba tofu can significantly increase the elasticity of Chiba tofu and make Chiba tofu of better quality.

The results of the sensory evaluation of each Chiba tofu by 20 food majors trained in specialized courses are shown in Figures (C,D). Figure (C) shows the radar chart of various sensory evaluations of each Chiba tofu, and Figure (D) is the

histogram of the total scores of each Chiba tofu sensory evaluation; it can be learned from Figures (C,D) that the texture, elasticity, color, and tissue state of the Chiba tofu made from the SPI after the ultrasound treatment with 200 W are better than those made from unmodified SPI, and similar to those of two brands of commercially available tofu, taste, elasticity, color, and tissue state are all the better than that of the unmodified SPI and can be similar to the two brands of soybean curd purchased in the market. Therefore, it can be concluded that the 200 W ultrasonic treatment of SPI in the production of Chiba tofu can improve the quality of Chiba tofu better.

#### 4. CONCLUSIONS

Overall, these results demonstrate that ultrasonic treatment at 200 W significantly enhances the functional properties of SPI by reducing the particle size, increasing the solubility, and improving the surface hydrophobicity and sulfhydryl content. Fluorescence and FT-IR analyses corroborate these changes, suggesting protein unfolding and structural modifications that lead to improved gelling ability, strength, and water retention capacity. The application of these findings to Chiba Tofu production illustrates the practical benefits of ultrasonic treatment including enhanced water retention, elasticity, and sensory quality. This work provides valuable insights into SPI modification strategies with the potential to broaden the application of soy proteins in food production.

#### ■ AUTHOR INFORMATION

##### Corresponding Authors

**Ziping Chen** – Anhui Promotion Center for Technology Achievements Transfer, Anhui Academy of Science and Technology, Hefei 230031, China; Anhui Province Product Quality Supervision and Inspection Institute, Hefei 230041, China; [orcid.org/0000-0003-4081-0916](https://orcid.org/0000-0003-4081-0916); Email: [zpchenhf@163.com](mailto:zpchenhf@163.com)

**Kefeng Zhai** – School of Biological and Food Engineering, Suzhou University, Suzhou 234000, China; Engineering Research Center for Development and High Value Utilization of Genuine Medicinal Materials in North Anhui Province, Suzhou 234000, China; [orcid.org/0000-0002-5198-4332](https://orcid.org/0000-0002-5198-4332); Email: [kefengzhai@163.com](mailto:kefengzhai@163.com)

##### Authors

**Xiao Wu** – School of Biological and Food Engineering, Suzhou University, Suzhou 234000, China; Engineering Research Center for Development and High Value Utilization of Genuine Medicinal Materials in North Anhui Province, Suzhou 234000, China

**Na Li** – School of Biological and Food Engineering, Suzhou University, Suzhou 234000, China; Anhui Promotion Center for Technology Achievements Transfer, Anhui Academy of Science and Technology, Hefei 230031, China

**Zeng Dong** – School of Biological and Food Engineering, Suzhou University, Suzhou 234000, China; Engineering Research Center for Development and High Value Utilization of Genuine Medicinal Materials in North Anhui Province, Suzhou 234000, China

**Qin Yin** – School of Biological and Food Engineering, Suzhou University, Suzhou 234000, China; Engineering Research Center for Development and High Value Utilization of Genuine Medicinal Materials in North Anhui Province, Suzhou 234000, China

**Marwan M. A. Rashed** – School of Biological and Food Engineering, Suzhou University, Suzhou 234000, China; Engineering Research Center for Development and High Value Utilization of Genuine Medicinal Materials in North Anhui Province, Suzhou 234000, China

**Lixiang Zhu** – School of Biological and Food Engineering, Suzhou University, Suzhou 234000, China

**Chuanlong Dan** – School of Biological and Food Engineering, Suzhou University, Suzhou 234000, China

**Xinyue Li** – School of Biological and Food Engineering, Suzhou University, Suzhou 234000, China

Complete contact information is available at:

<https://pubs.acs.org/10.1021/acsomega.4c06952>

#### Author Contributions

<sup>†</sup>X.W. and N.L. contributed equally to this work. Writing—original draft preparation, investigation, and formal analysis, X.W. and N.L.; methodology and investigation, Z.D. and Q.Y.; investigation, M.M.A.R., L.Z., C.D., and X.L.; and writing—review and editing, Z.C. and K.Z. All authors have read and agreed to the published version of the manuscript.

#### Notes

The authors declare no competing financial interest.

#### ■ ACKNOWLEDGMENTS

This study was supported by the Key Research Project of Anhui Education Department (grant Nos. 2023AH052239 and 2022AH051360), the Key Research Projects of Suzhou University (grant No. 2022yzd03), the Cross-cutting Projects at Suzhou University (grant No. 2023xhx258), and the Anhui Province Innovation Team of Authentic Medicinal Materials Development and High Value Utilization (grant No. 2022AH010080).

#### ■ REFERENCES

- (1) Bu, G.; Ren, M.; Zuo, Y.; Zhao, C. J. C. Functional characteristics and structural properties of soybean protein isolate–maltose conjugates. *Cereal Chem.* **2022**, *99* (1), 100–110.
- (2) Chen, B.; Zhao, X.; Cai, Y.; Jing, X.; Zhao, M.; Zhao, Q.; Van der Meeren, P. J. F. H. Incorporation of modified okara-derived insoluble soybean fiber into set-type yogurt: Structural architecture, rheological properties and moisture stability. *Food Hydrocolloids* **2023**, *137*, 108413.
- (3) Zheng, L.; Regenstein, J. M.; Zhou, L.; Wang, Z. Soy Protein Isolates: A Review of Their Composition, Aggregation, and Gelation. *Compr. Rev. Food Sci. Food Saf.* **2022**, *21* (2), 1940–1957.
- (4) Zhang, Z.; Wang, Y.; Jiang, H.; Dai, C.; Xing, Z.; Kumah Mintah, B.; Dabbour, M.; He, R.; Ma, H. J. U. S. Effect of dual-frequency ultrasound on the formation of lysinoalanine and structural characterization of rice dreg protein isolates. *Ultrason. Sonochem.* **2020**, *67*, 105124.
- (5) Frausto, D. M.; Forsyth, C. B.; Keshavarzian, A.; Voigt, R. M. J. F. i. n. Dietary regulation of gut-brain axis in Alzheimer's disease: Importance of microbiota metabolites. *Front. Neurosci.* **2021**, *15*, 736814.
- (6) Guo, A.; Xiong, Y. L. J. F. c. Glucose oxidase promotes gallic acid-myofibrillar protein interaction and thermal gelation. *Food Chem.* **2019**, *293*, 529–536.
- (7) Liang, G.; Chen, W.; Qie, X.; Zeng, M.; Qin, F.; He, Z.; Chen, J. Modification of Soy Protein Isolates Using Combined Pre-Heat Treatment and Controlled Enzymatic Hydrolysis for Improving Foaming Properties. *Food Hydrocolloids* **2020**, *105*, 105764.
- (8) Xu, J.; Yan, S.; Xu, J.; Qi, B. Ultrasound-Assisted Modification of Soybean Protein Isolate with L-Histidine: Relationship between Structure and Function. *Ultrason. Sonochem.* **2024**, *107*, 106934.

- (9) Ma, Z.; Li, L.; Wu, C.; Huang, Y.; Teng, F.; Li, Y. Effects of Combined Enzymatic and Ultrasonic Treatments on the Structure and Gel Properties of Soybean Protein Isolate. *LWT* **2022**, *158*, 113123.
- (10) Kang, Z.-L.; Zhang, X.-h.; Li, X.; Song, Z.-j.; Ma, H.-j.; Lu, F.; Zhu, M.-m.; Zhao, S.-m.; Wang, Z. r. J. J. o. f. s. The effects of sodium chloride on proteins aggregation, conformation and gel properties of pork myofibrillar protein Running Head: Relationship aggregation, conformation and gel properties. *J. Food Sci. Technol.* **2021**, *58*, 2258–2264.
- (11) Han, L.; Li, J.; Jiang, Y.; Lu, K.; Yang, P.; Jiang, L.; Li, Y.; Qi, B. Changes in the structure and functional properties of soybean isolate protein: Effects of different modification methods. *Food Chem.* **2024**, *432*, 137214.
- (12) Huang, L.; Ding, X.; Li, Y.; Ma, H. The Aggregation, Structures and Emulsifying Properties of Soybean Protein Isolate Induced by Ultrasound and Acid. *Food Chem.* **2019**, *279*, 114–119.
- (13) Wu, X.; Li, N.; Dong, Z.; Yin, Q.; Zhou, T.; Zhu, L.; Yan, H.; Chen, Z.; Zhai, K. J. F. Extraction, Purification, Sulfated Modification, and Biological Activities of Dandelion Root Polysaccharides. *Foods* **2024**, *13* (15), 2393.
- (14) Gharibzadeh, S. M. T.; Smith, B. The Functional Modification of Legume Proteins by Ultrasonication: A Review. *Trends Food Sci. Technol.* **2020**, *98*, 107–116.
- (15) Yan, S.; Xu, J.; Zhang, S.; Li, Y. Effects of Flexibility and Surface Hydrophobicity on Emulsifying Properties: Ultrasound-Treated Soybean Protein Isolate. *LWT* **2021**, *142*, 110881.
- (16) Wang, Z.; Zeng, L.; Fu, L.; Chen, Q.; He, Z.; Zeng, M.; Qin, F.; Chen, J. Effect of Ionic Strength on Heat-Induced Gelation Behavior of Soy Protein Isolates with Ultrasound Treatment. *Molecules* **2022**, *27* (23), 8221.
- (17) Liu, L.; Huang, Y.; Zhang, X.; Zeng, J.; Zou, J.; Zhang, L.; Gong, P. J. F. H. Texture analysis and physicochemical characteristics of fermented soymilk gel by different lactic acid bacteria. *Food Hydrocolloids* **2023**, *136*, 108252.
- (18) Liu, G.; Hu, M.; Du, X.; Liao, Y.; Yan, S.; Zhang, S.; Qi, B.; Li, Y. Correlating Structure and Emulsification of Soybean Protein Isolate: Synergism between Low-pH-Shifting Treatment and Ultrasonication Improves Emulsifying Properties. *Colloids Surf., A* **2022**, *646*, 128963.
- (19) Cui, Q.; Zhang, A.; Li, R.; Wang, X.; Sun, L.; Jiang, L. Ultrasonic Treatment Affects Emulsifying Properties and Molecular Flexibility of Soybean Protein Isolate-Glucose Conjugates. *Food Biosci.* **2020**, *38*, 100747.
- (20) Lu, Q.; Zuo, L.; Wu, Z.; Li, X.; Tong, P.; Wu, Y.; Fan, Q.; Chen, H.; Yang, A. J. F. C. Characterization of the protein structure of soymilk fermented by *Lactobacillus* and evaluation of its potential allergenicity based on the sensitized-cell model. *Food Chem.* **2022**, *366*, 130569.
- (21) Montemurro, M.; Pontonio, E.; Coda, R.; Rizzello, C. Plant-Based Alternatives to Yogurt: State-of-the-Art and Perspectives of New Biotechnological Challenges. *Foods* **2021**, *10*, 316.
- (22) Chen, Y.; Chen, M.; Luo, J.; Li, J.; Gao, Q. J. I. C. Effect of tannin on the bonding performance and mildew resistance of soybean meal-based adhesive. *Ind. Crop. Prod.* **2022**, *189*, 115740.
- (23) Dreher, J.; Blach, C.; Terjung, N.; Gibis, M.; Weiss, J. J. J. o. F. S. Formation and characterization of plant-based emulsified and crosslinked fat crystal networks to mimic animal fat tissue. *J. Food Sci.* **2020**, *85* (2), 421–431.
- (24) Li, J.; Li, X.; Wang, C.; Zhang, M.; Xu, Y.; Zhou, B.; Su, Y.; Yang, Y. Characteristics of Gelling and Water Holding Properties of Hen Egg White/Yolk Gel with NaCl Addition. *Food Hydrocolloids* **2018**, *77*, 887–893.
- (25) Gu, Z.; Liu, S.; Duan, Z.; Kang, R.; Zhao, M.; Xia, G.; Shen, X. J. J. o. t. S. o. F. Effect of citric acid on physicochemical properties and protein structure of low-salt restructured tilapia (*Oreochromis mossambicus*) meat products. *J. Sci. Food Agric.* **2021**, *101* (4), 1636–1645.
- (26) Li, R.; Cui, Q.; Wang, G.; Liu, J.; Chen, S.; Wang, X.; Wang, X.; Jiang, L. Relationship between Surface Functional Properties and Flexibility of Soy Protein Isolate-Glucose Conjugates. *Food Hydrocolloids* **2019**, *95*, 349–357.
- (27) Li, H.; Wang, Y.; Xie, W.; Tang, Y.; Yang, F.; Gong, C.; Wang, C.; Li, X.; Li, C. J. P. Preparation and characterization of soybean protein adhesives modified with an environmental-friendly tannin-based resin. *Polymers* **2023**, *15* (10), 2289.
- (28) Zhai, K.; Wang, W.; Zheng, M.; Khan, G.; Wang, Q.; Chang, J.; Dong, Z.; Zhang, X.; Duan, H.; Gong, Z.; Cao, H. Protective effects of Isodon Suzhouensis extract and glaucocalyxin A on chronic obstructive pulmonary disease through SOCS3–JAKs/STATs pathway. *Food Front.* **2023**, *4*, 511–523.
- (29) Feng, L.; Jia, X.; Zhu, Q.; Liu, Y.; Li, J.; Yin, L. Investigation of the Mechanical, Rheological and Microstructural Properties of Sugar Beet Pectin /Soy Protein Isolate-Based Emulsion-Filled Gels. *Food Hydrocolloids* **2019**, *89*, 813–820.
- (30) Sun, X.; Cui, Q.; Li, R.; Hao, L.; Liu, H.; Wang, X.; Xu, N.; Zhao, X. Structural and Emulsifying Properties of Soybean Protein Isolate Glycated with Glucose Based on pH Treatment. *J. Sci. Food Agric.* **2022**, *102* (11), 4462–4472.
- (31) Xu, X.; Li, L.; Zhang, H.; Sun, L.; Jia, B.; Yang, H.; Zuo, F. Interaction Mechanism between Soybean Protein Isolate and Citrus Pectin. *J. Food Sci.* **2022**, *87* (6), 2538–2548.
- (32) Li, N.; Wu, X.; Yin, Q.; Dong, Z.; Zheng, L.; Qian, Y.; Sun, Y.; Chen, Z.; Zhai, K. J. F. Extraction, Identification, and Antioxidant Activity of Flavonoids from *Hylotelephium spectabile* (Boreau) H. Ohba. *Foods* **2024**, *13* (17), 2652.
- (33) Alu'datt, M. H.; Rababah, T.; Kubow, S.; Alli, I. Molecular Changes of Phenolic-Protein Interactions in Isolated Proteins from Flaxseed and Soybean Using Native-PAGE, SDS-PAGE, RP-HPLC, and ESI-MS Analysis. *J. Food Biochem.* **2019**, *43* (5), No. e12849.
- (34) Wang, F.; Gu, X.; Lü, M.; Huang, Y.; Zhu, Y.; Sun, Y.; Zhu, X. Structural Analysis and Study of Gel Properties of Thermally-Induced Soybean Isolate–Potato Protein Gel System. *Foods* **2022**, *11* (22), 3562.
- (35) Zhang, M.; Yang, Y.; Acevedo, N. C. Effects of Pre-Heating Soybean Protein Isolate and Transglutaminase Treatments on the Properties of Egg-Soybean Protein Isolate Composite Gels. *Food Chem.* **2020**, *318*, 126421.
- (36) Zheng, L.; He, M.; Zhang, X.; Regenstein, J. M.; Wang, Z.; Ma, Z.; Kong, Y.; Wu, C.; Teng, F.; Li, Y. Gel Properties and Structural Characteristics of Soy Protein Isolate Treated with Different Salt Ions before Spray Drying Combined with Dynamic High-Pressure Microfluidization. *Food Bioprod. Process.* **2021**, *125*, 68–78.
- (37) Ingrassia, R.; Bea, L. L.; Hidalgo, M. E.; Risso, P. H. Microstructural and Textural Characteristics of Soy Protein Isolate and Tara Gum Cold-Set Gels. *LWT* **2019**, *113*, 108286.
- (38) Yang, X.; Ke, C.; Li, L. Physicochemical Rheological and Digestive Characteristics of Soy Protein Isolate Gel Induced by Lactic Acid Bacteria. *J. Food Eng.* **2021**, *292*, 110243.
- (39) Chen, X.; Yuan, J.; Li, R.; Kang, X. Characterization and Embedding Potential of Bovine Serum Albumin Cold-Set Gel Induced by Glucono- $\delta$ -Lactone and Sodium Chloride. *Food Hydrocolloids* **2019**, *95*, 273–282.
- (40) Zhang, M.; Li, J.; Su, Y.; Chang, C.; Li, X.; Yang, Y.; Gu, L. Preparation and Characterization of Hen Egg Proteins-Soybean Protein Isolate Composite Gels. *Food Hydrocolloids* **2019**, *97*, 105191.
- (41) Pang, H.; Yan, Q.; Ma, C.; Zhang, S.; Gao, Z. J. A. A. M. Polyphenol-Metal Ion Redox-Induced Gelation System for Constructing Plant Protein Adhesives with Excellent Fluidity and Cold-Pressing Adhesion. *ACS Appl. Mater. Interfaces* **2021**, *13* (49), 59527–59537.
- (42) Xu, Z.; Bera, H.; Wang, H.; Wang, J.; Cun, D.; Feng, Y.; Yang, M. J. A. M. M. Inhalable ciprofloxacin/polymyxin B dry powders in respiratory infection therapy. *Acta Mater. Med.* **2023**, *2* (2), 142–156.
- (43) Huang, Z.; Sun, J.; Zhao, L.; He, W.; Liu, T.; Liu, B. Analysis of the Gel Properties, Microstructural Characteristics, and Intermolec-

ular Forces of Soybean Protein Isolate Gel Induced by Transglutaminase. *Food Sci. Nutr.* **2022**, *10* (3), 772–783.

(44) Gradzielski, M. Polymer–surfactant interaction for controlling the rheological properties of aqueous surfactant solutions. *Curr. Opin. Colloid Interface Sci.* **2023**, *63*, 101662.

(45) Lu, Y.; Zhang, Y.; Yuan, F.; Gao, Y.; Mao, L. Emulsion Gels with Different Proteins at the Interface: Structures and Delivery Functionality. *Food Hydrocolloids* **2021**, *116*, 106637.

(46) Kang, Z.-L.; Zhang, X.; Li, X.; Song, Z.; Ma, H.; Lu, F.; Zhu, M.; Zhao, S.; Wang, Z. The Effects of Sodium Chloride on Proteins Aggregation, Conformation and Gel Properties of Pork Myofibrillar Protein Running Head: Relationship Aggregation, Conformation and Gel Properties. *J. Food Sci. Technol.* **2021**, *58* (6), 2258–2264.

(47) Picchio, M. L.; Linck, Y. G.; Monti, G. A.; Gugliotta, L. M.; Minari, R. J.; Alvarez Igarzabal, C. I. Casein films crosslinked by tannic acid for food packaging applications. *Food Hydrocolloids* **2018**, *84*, 424–434.

(48) Tokay, F. G.; Alp, A. C.; Yerlikaya, P. J. J. o. A. F. P. T. RSM Based Process Variables Optimization of Restructured Fish Meat. *J. Aquat. Food Prod. Technol.* **2022**, *31* (8), 828–841.

(49) Yin, M.; Yang, D.; Lai, S.; Yang, H. Rheological Properties of Xanthan-Modified Fish Gelatin and Its Potential to Replace Mammalian Gelatin in Low-Fat Stirred Yogurt. *LWT* **2021**, *147*, 111643.

(50) Lin, D.; Zhang, L.; Li, R.; Zheng, B.; Rea, M. C.; Miao, S. Effect of Plant Protein Mixtures on the Microstructure and Rheological Properties of Myofibrillar Protein Gel Derived from Red Sea Bream (*Pagrosomus Major*). *Food Hydrocolloids* **2019**, *96*, 537–545.

(51) Wang, T.; Wang, N.; Yu, Y.; Yu, D.; Xu, S.; Wang, L. J. F. H. Study of soybean protein isolate-tannic acid non-covalent complexes by multi-spectroscopic analysis, molecular docking, and interfacial adsorption kinetics. *Food Hydrocolloids* **2023**, *137*, 108330.

(52) Yang, H.; Wang, S.; Xu, Y.; Wang, S.; Yang, L.; Song, H.; He, Y.; Liu, H. J. F. c. Storage stability and interfacial rheology analysis of high-internal-phase emulsions stabilized by soy hull polysaccharide. *Food Chem.* **2023**, *418*, 135956.

(53) Zhao, C.; Chu, Z.; Mao, Y.; Xu, Y.; Fei, P.; Zhang, H.; Xu, X.; Wu, Y.; Zheng, M.; Liu, J. Structural Characteristics and Acid-Induced Emulsion Gel Properties of Heated Soy Protein Isolate–Soy Oligosaccharide Glycation Conjugates. *Food Hydrocolloids* **2023**, *137*, 108408.

(54) Li, J.; Wang, K.; Gao, Y.; Ma, C.; Sun, D.; Hussain, M. A.; Qayum, A.; Jiang, Z.; Hou, J. Effect of Thermal Treatment and Pressure on the Characteristics of Green Soybean Tofu and the Optimization Conditions of Tofu Processing by TOPSIS Analysis. *LWT* **2021**, *136*, 110314.

(55) Yang, X.; Jiang, S.; Li, L. The Gel Properties and Gastric Digestion Kinetics of a Novel Lactic Acid Bacteria Fermented Tofu: Focusing on the Effects of Transglutaminase. *LWT* **2021**, *143*, 110998.

(56) Zheng, L.; Wang, Z.; Kong, Y.; Ma, Z.; Wu, C.; Regenstein, J. M.; Teng, F.; Li, Y. Different Commercial Soy Protein Isolates and the Characteristics of Chiba Tofu. *Food Hydrocolloids* **2021**, *110*, 106115.

(57) Yang, X.; Zhang, Y. J. F. C. Expression of recombinant transglutaminase gene in *Pichia pastoris* and its uses in restructured meat products. *Food Chem.* **2019**, *291*, 245–252.

(58) Li, N.; Hamor, C.; An, Y.; Zhu, L.; Gong, Y.; Toh, Y.; Guo, Y. R. Biological Functions and Therapeutic Potential of Acylation by Histone Acetyltransferases. *Acta Mater. Med.* **2023**, *2*, 228–254.

(59) Liu, S. X.; Chen, D.; Plumier, B.; Berhow, M.; Xu, J.; Byars, J. A. Impact of Particle Size Fractions on Composition, Antioxidant Activities, and Functional Properties of Soybean Hulls. *J. Food Meas. Char.* **2021**, *15* (2), 1547–1562.

(60) Li, J.; Wang, B.; Fan, J.; Zhong, X.; Huang, G.; Yan, L.; Ren, X. Foaming, Emulsifying Properties and Surface Hydrophobicity of Soy Proteins Isolate as Affected by Peracetic Acid Oxidation. *Int. J. Food Prop.* **2019**, *22*, 689–703.

(61) Chen, Y.-B.; Zhu, X.-F.; Liu, T.-X.; Lin, W.-F.; Tang, C.-H.; Liu, R. Improving Freeze-Thaw Stability of Soy Nanoparticle-Stabilized Emulsions through Increasing Particle Size and Surface Hydrophobicity. *Food Hydrocolloids* **2019**, *87*, 404–412.

(62) Zhang, X.; Lu, P.; Xue, W.; Wu, D.; Wen, C.; Zhou, Y. An Evaluation of Heat on Protein Oxidation of Soy Protein Isolate or Soy Protein Isolate Mixed with Soybean Oil in Vitro and Its Consequences on Redox Status of Broilers at Early Age. *Asian-Australas. J. Anim. Sci.* **2017**, *30* (8), 1135–1142.

(63) Ren, X.; Li, C.; Yang, F.; Huang, Y.; Huang, C.; Zhang, K.; Yan, L. Comparison of Hydrodynamic and Ultrasonic Cavitation Effects on Soy Protein Isolate Functionality. *J. Food Eng.* **2020**, *265*, 109697.

(64) He, M.; Li, L.; Wu, C.; Zheng, L.; Jiang, L.; Huang, Y.; Teng, F.; Li, Y. Effects of Glycation and Acylation on the Structural Characteristics and Physicochemical Properties of Soy Protein Isolate. *J. Food Sci.* **2021**, *86* (5), 1737–1750.

(65) Stephan, M. P.; Felberg, I.; Carrão-Panizzi, M. Electrophoresis SDS-PAGE and Tricine-SDS-PAGE to Differentiate Black and Yellow Soybean: A Molecular Approach. *South Fla. J. Dev.* **2021**, *2* (2), 2592–2599.

(66) Liu, C.; Wang, N.; Wu, D.; Wang, L.; Zhang, N.; Yu, D. Rapid Quantitative Analysis of Soybean Protein Isolates Secondary Structure by Two-Dimensional Correlation Infrared Spectroscopy through pH Perturbation. *Food Chem.* **2024**, *448*, 139074.

(67) Ningtyas, D. W.; Tam, B.; Bhandari, B.; Prakash, S. Effect of Different Types and Concentrations of Fat on the Physico-Chemical Properties of Soy Protein Isolate Gel. *Food Hydrocolloids* **2021**, *111*, 106226.

(68) Baydin, T.; Arntsen, S. W.; Hattrem, M. N.; Draget, K. I. Physical and Functional Properties of Plant-Based Pre-Emulsified Chewable Gels for the Oral Delivery of Nutraceuticals. *Appl. Food Res.* **2022**, *2* (2), 100225.

(69) Yao, Y.; He, W.; Xu, B. Physicochemical Characteristics and Sensory Properties of Plant Protein Isolates–Konjac Glucomannan Compound Gels. *Food Sci. Nutr.* **2023**, *11* (9), 5063–5077.

(70) Zhang, P.; Bao, Z.; Wang, H.; Tu, Z.; Sha, X.; Hu, Y. Ultrasonic Pretreatment Improved the Physicochemical Properties and Riboflavin Delivery Ability of Transglutaminase-Catalyzed Soy Protein Isolate Gel. *Food Hydrocolloids* **2022**, *131*, 107782.

(71) Saavedra Isusi, G. I.; Paz Puga, D.; van der Schaaf, U. S. Texturing Fermented Emulsion Gels from Soy Protein: Influence of the Emulsifying Agent—Soy Protein vs. Pectin Microgels—On Gel Microstructure, Rheology and Tribology. *Foods* **2022**, *11* (3), 294.